

ARE CORONAE OF LATE-TYPE STARS MADE OF SOLAR-LIKE STRUCTURES? THE X-RAY SURFACE FLUX VERSUS HARDNESS RATIO DIAGRAM AND THE PRESSURE-TEMPERATURE CORRELATION

G. PERES

Dipartimento di Scienze Fisiche ed Astronomiche, Sezione di Astronomia, Piazza del Parlamento 1, 90134 Palermo, Italy;
peres@oapa.astropa.unipa.it

S. ORLANDO

INAF, Osservatorio Astronomico “G. S. Vaiana,” Piazza del Parlamento 1, 90134 Palermo, Italy; orlando@oapa.astropa.unipa.it

AND

F. REALE

Dipartimento di Scienze Fisiche ed Astronomiche, Sezione di Astronomia, Piazza del Parlamento 1, 90134 Palermo, Italy;
reale@oapa.astropa.unipa.it

Received 2003 May 13; accepted 2004 May 10

ABSTRACT

This work is dedicated to the solar-stellar connection, i.e., the close similarity of the Sun and late-type stars; in particular, this work shows that stellar coronae can be composed of X-ray-emitting structures similar to those present in the solar corona. To this end we use a large set of *ROSAT* PSPC observations of late-type stars of all spectral types and activity levels and a large set of solar X-ray data collected with *Yohkoh* SXT. Solar data have been analyzed and formatted to study the Sun as an X-ray star; they include observations of the solar corona at various phases of the solar cycle and data on various kinds of X-ray coronal structures, from flares to the background corona, i.e., the most quiet regions. We use the X-ray surface flux (F_X) versus spectral hardness ratio (HR) diagram as a fundamental tool for our study. We find that F_X is strongly correlated to HR in stellar coronae, in the solar corona at all phases of the solar cycle, and in the individual solar coronal structures; all the above follow the same law. Schmitt found the same correlation in stellar coronae. We therefore claim that coronae of late-type stars are formed with X-ray structures very similar to those in the Sun, since their behavior is identical to that of the solar coronal structures and of the whole solar corona. The spatial location of the X-ray structures on the star, however, could be very different from those on the Sun. In this scenario, the fraction of the stellar surface covered with active regions and their bright cores increases with activity; the most active stars are brighter and hotter than if they were entirely covered with active regions, so they can be explained only with the additional presence of several flares (or flarelike structures) at any time. On the basis of the F_X versus HR correlation, corresponding to $F_X \propto T^6$, we then derive a set of new laws relating the temperature, pressure, volumetric heating, and characteristic loop length of the coronal plasma on all the late-type stars. In addition, individual solar coronal structures and the whole solar corona follow the same laws. These laws also agree with recent findings of higher plasma density at higher temperatures in stellar coronae. We claim that the strong correlation between surface flux and temperature and the laws mentioned above are just the effect of more fundamental physical mechanisms driving the coronal structures of all the late-type stars from the emergence of new magnetic structures to their dispersal and dissipation.

Subject headings: stars: coronae — Sun: corona — Sun: X-rays, gamma rays — X-rays: stars

1. INTRODUCTION

Since the seminal work by Vaiana et al. (1981), it has become clear that all late-type stars share the same basic coronal characteristics: the presence of thermal plasma at several million degrees, magnetic confinement, the presence of flares, etc. The basic plasma physics governing coronae is also probably very similar in all these stars. On the other hand, coronae cover a large range of X-ray luminosity (even among stars of the same spectral type and luminosity class), and a few scientists think that the coronae of the most active late-type stars are different from the solar corona, although the crucial differences have rarely been stated clearly.

Two otherwise identical stars may have rather different levels of stellar activity, i.e., X-ray luminosity, spottedness, UV luminosity, etc., because of very different rotation speed (Pallavicini et al. 1981) and age (for reviews on the subject see Micela 2002a, 2002b); the speed probably determines how effectively the stellar magnetic dynamo generates magnetic fields.

One might then expect that many differences among the coronae of late-type stars are just due to rather different regimes of the dynamo at work inside stars, while the basic plasma phenomena occurring in the outer magnetized coronal plasma are probably the same, only differing in amount and scale. Along this line of thought, this work explores to what extent most of the differences found among the various coronae can be attributed to their different composition in terms of various kinds of coronal structures (ranging from the relatively faint and cool structures of the background corona to the very bright and hot flaring regions) and to the number of X-ray-emitting coronal structures present; on the other hand, we explore to what extent the plasma phenomena and the structures involved in the coronae are similar even in stars of very different activity levels. According to this paradigm, the solar corona offers the opportunity to study and better understand the building blocks of any late-type star's corona. To this end we compare the average surface flux (F_X) and the spectral hardness ratio (HR) in the *ROSAT* PSPC band of late-type stars

with those of solar coronal structures; we also study the strong F_X -HR correlation (Schmitt 1997, hereafter S97).

In the following discussion we do not claim that all the aspects of the solar corona are the same as in the coronae of late-type stars, but only that the fundamental features are the same; for instance, there is evidence of polar active regions (ARs) and large polar flares (e.g., Schmitt & Favata 1999; Brickhouse et al. 2001; see also Schrijver & Title 2001). We concentrate on the X-ray emission from stellar coronae and compare the solar and the various stellar cases, and through analogies and differences we infer (or just constrain) features of X-ray emitting structures present in stellar coronae.

A few works along this line of thought have been published, either studying the temperature versus emission measure per unit area on active stars (Schrijver et al. 1984; Jordan & Montesinos 1991) or correlating activity parameters (e.g., luminosity in given bands or emission measure) with temperature (Schmitt et al. 1990; Guedel et al. 1997; Preibisch 1997). In more detail, Schrijver et al. (1984) analyzed a sample of 34 late-type stars observed with the *Einstein* telescope and related the relevant coronal temperature and emission measure per unit area and rotation rate, determining scaling laws among these parameters and relating the first two through loop models. Jordan & Montesinos (1991) studied various scalings among emission measure, coronal temperature, surface gravity, and Rossby number. Schmitt et al. (1990) performed an extensive survey of late-type stars observed with the *Einstein* telescope, studying and relating the coronal features and showing some differences among M stars, F and G stars, giants, and RS CVn stars. Guedel et al. (1997) studied the “X-Ray Sun in Time” with the help of various X-ray observations of solar-like stars of different ages; they found a power-law dependence of the total X-ray luminosity on the temperature of the hottest component of a two-temperature spectral fit. Preibisch (1997) studied a sample of young late-type stars and found a power-law dependence of total X-ray luminosity on the temperature of the hottest component.

This work is based on methods and results developed in our program to study the solar-stellar connection in X-rays, mostly based on *ROSAT* PSPC and *Yohkoh* SXT data. Our approach allows us to directly link, with just a little elaboration and interpretation, the vast amount of data collected with these two observatories. In addition, our method and scope is novel in that we use solar data (made compatible with stellar data) as a template and a guide. Our findings are eventually interpreted in terms of coronal loop scaling laws. *ROSAT* has provided the largest homogeneous data set of stellar coronal observations so far collected; this data set is an important reference for studies of stellar coronae, because (1) the relevant data have been collected with just one instrument, (2) instrumental and observing conditions were relatively stable, (3) a large number of stars of different spectral types and luminosity classes have been observed, and (4) the data set has an extended time coverage. For analogous reasons, *Yohkoh* SXT data are equally important to studying the solar corona. It is, therefore, natural to refer both to *ROSAT* and to *Yohkoh* data in order to model a scenario of coronae of late-type stars and to connect it to the solar corona. In the following discussion we also use results of previous works on the solar-stellar connection in the X-ray band plus some stellar data already published in different contexts; our scope is to draw a global picture of coronal structure.

The paper is organized as follows: § 2 describes our method to use the solar corona as a template to study stellar coronae, § 3 presents and discusses some of the related results along

with related works on stellar X-ray emission, and in § 4 we draw our conclusions.

2. THE “SUN AS AN X-RAY STAR” PROGRAM

The scope of this program has been to study the X-ray emission of the whole Sun as an X-ray star and the contribution of the various coronal structures to its emission using *Yohkoh* SXT data; we have translated the solar observations into a format similar to those of stellar observations. Thanks to this approach, we can now easily perform comparative studies among solar and stellar observations.

Yohkoh SXT data have relatively high time resolution, down to a few seconds, and continuously cover ~ 10 yr, from the maximum of the solar cycle in 1991 to the following one. All sorts of phenomena have been observed, ranging from extremely large flares to moments of very low emission during the cycle minimum. The spatial resolution (typically $\sim 5''$) allows us to identify and study, with high spatial detail, the various originating regions of the X-ray emission and to discriminate, as well as to isolate, the contribution of different coronal structures to the coronal X-ray emission.

In brief, from the *Yohkoh* SXT images of the Sun at a given time, we derive a 512×512 pixel map of coronal plasma temperature and a corresponding map of emission measure. From there we derive the distributions of coronal emission measure versus temperature at each observation time. Then by summing the optically thin spectrum emitted at each temperature (obtained with the corresponding emission measure value and a spectral synthesis code), we obtain the spectrum of the whole corona. Folding it with the known instrumental characteristics (effective area vs. photon energy and photon redistribution matrix), we derive the stellar-like focal plane spectrum of the Sun, as it would be observed with the X-ray telescope of interest (Orlando et al. 2000, hereafter Paper I; Peres et al. 2000, hereafter Paper II). In this work we focus on the *ROSAT* PSPC data set and use the *ROSAT* standard data analysis to analyze solar data translated into stellar format and conditions.

The capability to isolate the various kinds of coronal structures has allowed us to study their conditions and their contributions to the coronal spectrum (for the flares, see Reale et al. 2001, hereafter Paper III; for the background corona, the ARs, and the cores of ARs, see Orlando et al. 2001, hereafter Paper IV). The good time coverage of *Yohkoh* SXT observations has been exploited to study how the emission measure distribution and the X-ray spectrum of the whole corona change during the solar cycle, with a regular time sampling and taking care not to include flare events (Papers II and IV).

3. THE F_X -HR DIAGRAMS

3.1. *The Diagrams with Stellar Data*

S97 presented the results of a large set of *ROSAT* PSPC observations of late-type stars within 13 pc from the Sun in the form of a diagram (Fig. 1) of F_X (the average X-ray surface flux of the star) versus HR (the X-ray spectral hardness ratio). The hardness ratio is defined as $HR = (H - S)/(H + S)$, where H is the total flux in the *ROSAT* PSPC spectral channels between 0.55 and 1.95 keV and S is the total flux in the channels between 0.13 and 0.40 keV. It is a simple characterization of the relative weight of the hard and soft part of the spectrum.¹

¹ It is worth noting that we have omitted from the sample of S97 stars those with $HR \approx -1$, i.e., $T \approx 10^6$ K, since the HR becomes inadequate (see also Fig. 2); also, small HR errors around that temperature yield large temperature errors.

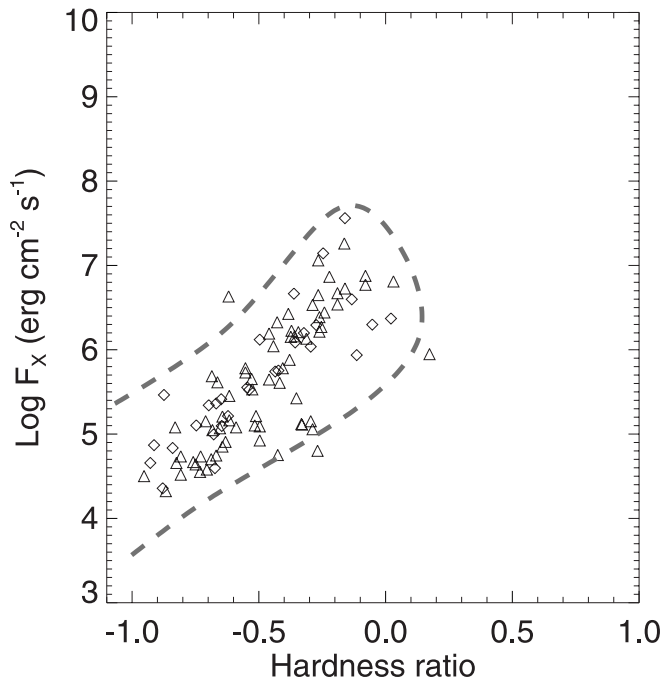


FIG. 1.— F_X vs. HR diagram (see text for details) adapted from Schmitt (1997) of a large set of late-type stars observed with *ROSAT* PSPC. Diamonds identify F- and G-type stars and triangles K and M stars. The dashed area marks the strip covered by late-type stars in Schmitt (1997) for ease of comparison with the following graphs. We have omitted the stars with $HR \approx -1$ from Schmitt (1997) because their temperatures are not well determined.

Both F_X and HR are useful to characterize the strength of coronal activity, albeit averaged over the whole corona. Indeed, F_X gives the coronal radiative losses of the star per unit area and is related to the amount of energy delivered into the corona, i.e., the coronal heating, also per unit area. It can discriminate between two stars of the same X-ray luminosity but of very different radius and surface area: the smaller star will have a much higher flux than the other, hinting at a much higher level of plasma activity. F_X is an activity marker independent of the stellar surface value. HR is a simple tracer, albeit a nonlinear one, of the coronal average temperature. It is another index of plasma activity, independent of F_X .

Figure 2 shows the relationship between the plasma temperature and the HR of the spectrum derived with the MEKAL (Mewe et al. 1986; Kaastra 1992; Mewe et al. 1995 and references therein) spectral synthesis model. Note that HR is not very sensitive to temperatures below 10^6 K; it also saturates and is multivalued in the range 0.0–0.4. Therefore, HR is also relatively insensitive to very hot plasma. Moreover, HR should not go beyond 0.4 at any plasma temperature.

The S97 results show that late-type stars cover a diagonal strip with HR ranging from -1.0 to 0.0 and F_X from 10^4 to 10^8 ergs $\text{cm}^{-2} \text{s}^{-1}$ (Fig. 1). The more active a star, the higher are both its F_X and its HR; the highest HR (temperature) and F_X values belong to uncommonly active stars. The overall trend suggests that the confined plasma in the corona of a late-type star, on the average, gets brighter as it gets hotter.

Analogously, Marino et al. (2002b) reported the data of 40 late-type stars of spectral type between F7 and K2 within 25 pc from the Sun in an analogous F_X versus HR diagram, shown in Figure 3. The stars of this sample are, on the average, more luminous and active than those in S97; also, differently from S97, M and late K stars were not included. There were 70 pointed *ROSAT* PSPC observations; some of these stars were

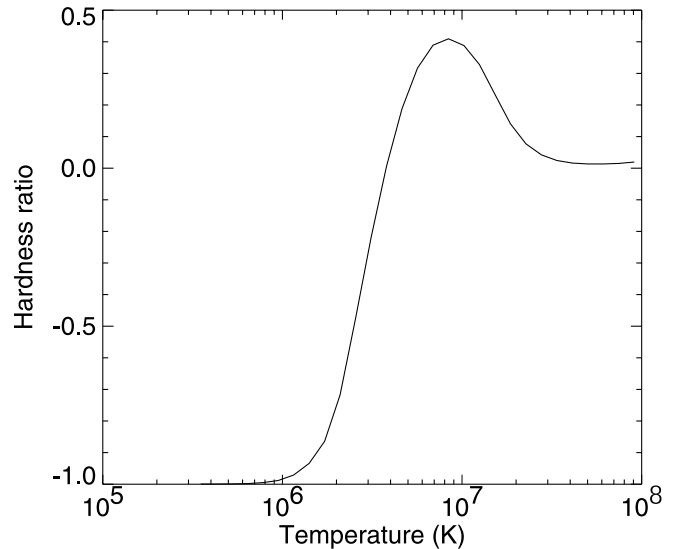


FIG. 2.—HR (hardness ratio) of the spectrum of a hot single-temperature coronal plasma detected with *ROSAT* PSPC vs. the plasma temperature.

observed several times, and some observations of sufficient signal-to-noise ratio were split to allow time-resolved analysis during the observation. Some of these stars moved in time along the same diagonal track where most of the stars are located; however, some stars evolved along a path in this graph that is less steep; we suggest below that this different evolution may be due to the contribution of flares. Steltzer (2001) also generated preliminary F_X versus HR diagrams for stars in clusters.

3.2. The Diagrams with Solar Data

In Paper II we studied the solar corona at the maximum, at an intermediate phase, and at the minimum of the solar cycle, taking care not to include flare events; the whole solar corona

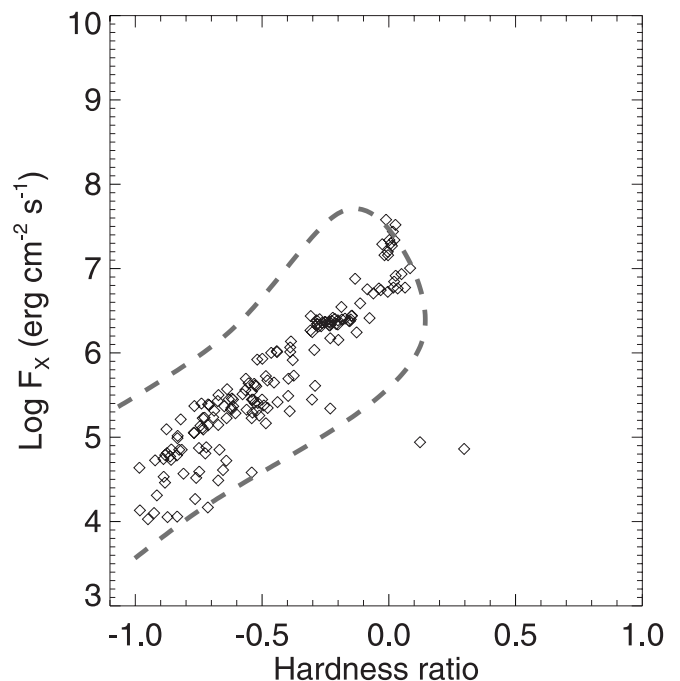


FIG. 3.—Results from Marino et al. (2002b) for dF7–dK2 stars, shown similarly to Fig. 1.

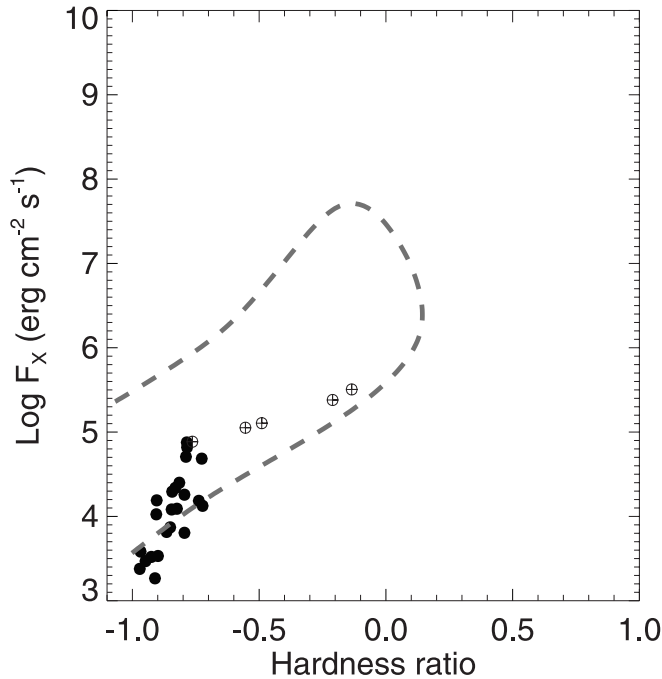


FIG. 4.— F_X -HR diagram of the whole solar corona along the solar cycle. The data points yield F_X and HR values averaged over the whole Sun; *filled circles*, the solar cycle from maximum (highest values) to minimum (lowest ones); *circled crosses*, the whole solar corona during an X9 flare (i.e., the evolution of the flare plus the steady nonflaring corona). Data are from Peres et al. (2000) and Orlando et al. (2001, 2004).

during a large flare event was also studied. Paper III was entirely dedicated to study, with the same method, the evolution of eight representative flare events ranging from small to large and covering most of the conditions encountered in flares; each flaring region was studied separately from the rest of the corona, so the surface flux and the HR were derived just for the flaring region, and its effect was not added to, and thus not diluted within, the whole corona.

Paper IV studied the solar corona at several moments of the solar cycle, sampling the cycle better than in Paper II and separately studying the various classes of coronal structures, classified as background corona (very quiet regions), ARs, and cores of ARs according to their surface brightness in *Yohkoh* SXT bands. The whole set of data mentioned above yields a good sampling of the physical conditions in the corona from the background corona to the strongest flares and spans the whole solar cycle.

For the present work we have taken all the flares in the sample of Paper III, because they are well observed, so they can be studied and characterized accurately; also, since they span a large range within the flare classification and the various phases of their evolution are well observed, they provide a good sampling of the various conditions encountered in flares, from the largest down to very small events. Most of our attention is focused on the physical conditions of various flare phases. We did not consider microflares, because they can hardly be discriminated from small AR variability, and their contribution in the context of average stellar F_X and HR is, in practice, the same as that from bright ARs.

Figure 4 shows a F_X -HR graph of the whole solar corona during the solar cycle plus the evolution of the whole solar corona near the maximum of the cycle in the course of an X9 flare; the graph collects some results of Paper II, Paper IV, and Orlando et al. (2002). The flux of the whole solar corona was

derived by dividing the total coronal luminosity by the whole solar surface area.

The evolution of the whole solar corona along the solar cycle, apart from moderate to large flares, spans the lower part of the diagram, the same as that covered by low-activity stars, i.e., the ones at low F_X and low HR, well below the levels of most active stars.² Solar flares span quite a large range, from very faint and barely detectable to very large ones; the flares included in our work are those that at least triggered the *Yohkoh* flare mode; in this respect they can be considered to be representative of flares from moderate to large. If a moderate to large flare happens at the maximum of the cycle, it makes the luminosity (and the flux) of the solar corona change at most by a factor ~ 2 during large flares. However, the corresponding increase of HR can be larger than the changes occurring along the solar cycle for the same increase of luminosity. Analogous flares occurring during the solar minimum carry a similar change in HR but a much larger change of luminosity and flux. Thus, under the effect of significant flares, the whole Sun moves rightward in the graph, on a path less steep than that covered by stars of various activity levels.

The occurrence of large flares may explain why the evolution of some stars studied by Marino et al. (2002b) follows a path in this diagram that is less steep than the track of all the other stars: although they show no evidence of large changes of flux, they may undergo a moderate flaring episode, which shows up through the HR change and the different path of the star in the diagram (see also Orlando et al. 2002, 2003).

Figure 5 shows F_X versus HR for four specific classes of structures (i.e., background corona, ARs, cores of ARs, and flares). It is worth noting that the flux has been derived by dividing the luminosity of the structure (or of the structures of that class) by the surface covered in *Yohkoh* SXT images.

The interpretation of these results is useful for stellar physics: a star entirely covered with solar-like ARs would be in the same part of the F_X -HR diagram as solar ARs, and the same would be true for all the other kinds of structures, since they would yield the same HR (average temperature) and surface flux values. Therefore, we can foresee how differently a stellar corona would behave if covered with the various kinds of solar coronal structures. More generally, however, a mixture of two different classes of structures would yield values intermediate between the two, with the effective value depending on the relative fractions of stellar surface covered. Interestingly enough, solar structures of different kinds (with the exception of solar flares) span the same region of the graph covered by stellar coronae of different activity levels. Quite likely the stellar surface is not entirely covered with X-ray emitting structures, and different classes of structures (according to our classification) do coexist on the star, covering different fractions of its surface. While places at the extremes of the graph can most likely be explained with only one kind of structure, a locus between two classes of structures could be explained with an appropriate (nonlinear) combination of the two. It is worth noting that, according to the analogy we are drawing here, a star equivalent to a structure, e.g., an AR, would be located in the same place in the diagram if it were fully covered by this type of structure; similarly, a star intermediate

² *Yohkoh* SXT most likely underestimates the emission of plasma with a temperature around 10^6 K or lower as well as the relevant emission measure, while the same plasma would have significant emission in the *ROSAT* PSPC band (see Judge et al. 2003). The solar data points relative to background corona and/or the very quiet Sun at cycle minimum may have to be shifted at higher flux; this effect is not crucial, however, in the context of this paper.

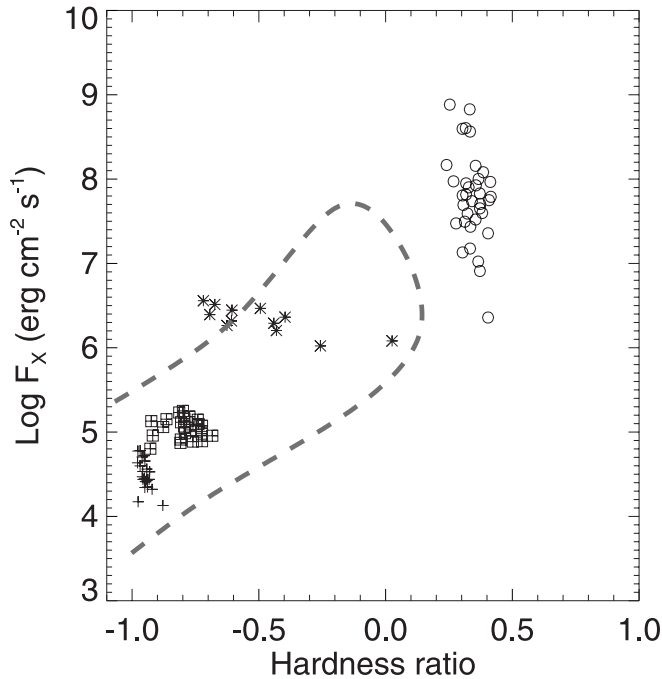


FIG. 5.— F_X -HR diagram of various kinds of structures present in the solar corona: background corona (*crosses*); active regions (*squares*); cores of active regions (*asterisks*); and flares (*circles*). Data on flares are from Reale et al. (2001); all the others are from Orlando et al. (2001).

between two kinds of structures should have its surface close to 100% covered with the two kinds of structures. In the solar case we know from *Yohkoh* SXT observations that ARs, their cores, and flares (when they occur) cover a small fraction of the surface of the Sun, while the rest is covered by the very faint background corona (as shown by very long exposure images). S97 has shown that very faint coronae have a surface flux comparable to that of very faint solar background corona. We can therefore imagine that on active stars also a faint background corona covers the surface not covered by active structures.

On the basis of the above interpretation, then, we see that the coronae of stars with extremely low surface flux and hardness ratio could be just a large solar coronal hole, as S97 suggested. Continuing this exercise by increasing the fraction of stellar surface covered with ARs, with the cores of ARs, or with a combination of these, we find that the corona spans the strip covered by coronae of late-type stars from low to intermediate activity.

Therefore, we can draw a hypothesis according to which the levels of stellar coronal X-ray emission are due to different fractions of the stellar surface covered with ARs or even cores of young ARs. The fraction of more active components increases for coronae of higher F_X and higher HR, with one notable exception: the few very high F_X ($>10^{6.5}$ ergs $\text{cm}^{-2} \text{s}^{-1}$) and very high HR (>-0.3) late-type stars. The average characteristics of these few stars are beyond the peak values of the solar coronal ARs cores. Yet they are well below the conditions of solar flares of interest here. The most active late-type stars can therefore be explained as being partly covered with ARs, their cores, and with flares or flarelike (i.e., very hot and dense) structures at all times. Very active stars may then be continuously subject to several uncorrelated flares whose light curves overlap randomly, canceling most of the evidence of variability. Some authors have already proposed the presence

of continuous flaring activity in stellar coronae (Wood et al. 1997; Drake et al. 2000; Guedel et al. 2002 and references therein).

Flares can contribute to coronae of low activity on the strip as long as the flares are small; indeed, large flares in low-activity stars are very evident and make their F_X -HR point move along a path much less inclined than the strip, bringing them out of the strip itself. There appears to be no match in the solar corona for those superhot and superluminous flares detected on very active stars and on RS CVns with the *BeppoSAX* and *ASCA* satellites (Franciosini et al. 2001; Maggio et al. 2000; Favata et al. 2000; Favata & Schmitt 1999; Schmitt & Favata 1999).

3.3. Global Scaling Relations

The F_X -HR diagram provides information on the average features of the coronal loops forming the structures. The amount of energy emitted from the coronal part of any loop is approximately one-half of the entire heating of the loops per unit cross-sectional area (approximately equal to the part of the solar surface covered by the loop's footpoints), the other half is emitted from the transition region (Vesecy et al. 1979). Therefore, considering that F_X is proportional to the heating

$$F_X = KF_{\text{tot}} = KE_H L$$

and using the scaling laws by Rosner et al. (1978), hereafter RTV78, i.e.,

$$E_H = 10^5 p^{7/6} L^{-5/6} \quad (1)$$

and

$$T = 1.4 \times 10^3 (pL)^{1/3}, \quad (2)$$

we find

$$F_X = K' p^{7/6} L^{1/6} = K' p (pL)^{1/6} = K'' p T^{1/2},$$

where K , K' , and K'' are proportionality factors, F_{tot} is the total radiated flux, E_H is the heating per unit volume averaged along field lines, p is the coronal plasma pressure, T is the coronal loop maximum temperature, and L is the half-length of the magnetic loop. Then, given the very weak dependence on T , F_X is very close to being linearly related to the coronal pressure. A closer look at the above derivation shows that the linear relation between F_X and F_{tot} is appropriate only for a large part (but not all) of the temperature range, since one expects that for very high T (above a few 10^7 K) or very low T (below 10^6 K), different fractions of F_{tot} fall outside the *ROSAT* band. Nonetheless, the main point of the above exercise is to show that F_X variations are largely dominated by pressure variations. Of course, HR changes are related to temperature changes.

Using the simple relation derived above and the HR versus T relation in Figure 2, it is straightforward to translate the F_X versus HR diagram into an “average pressure” versus “average temperature” diagram, deriving the temperature from the single-valued part ($T < 4 \times 10^6$ K) of the hardness ratio and then the pressure as $p = F_X / (K'' T^{0.5})$. Figure 6 shows the pressure-temperature graphs for solar structures for the whole solar corona, for the F and G stars in S97, and for the G stars (from F7 to K2) in Marino et al. (2002b).

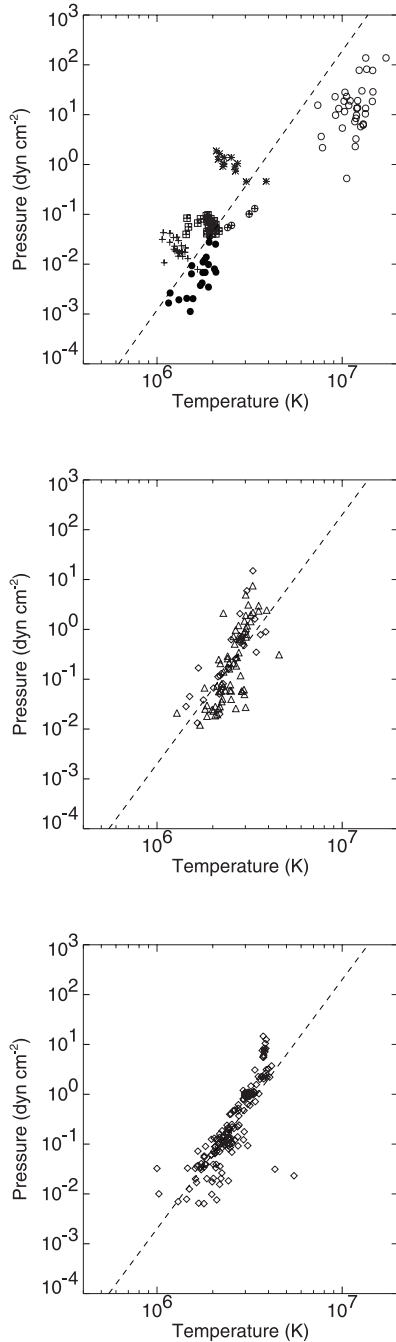


FIG. 6.—Pressure-temperature diagram for the stellar and the solar data shown in previous figures. *Top panel:* Whole solar corona during the cycle shown in Fig. 4, plus the various structures shown in Fig. 5. *Middle panel:* Stellar data from Schmitt (1997). *Bottom panel:* Stellar data from Marino et al. (2002b). Symbols are the same as in previous figures. *Dashed line:* The $p = (1.2 \times 10^{-3}) T_6^{5.2}$ fitting to the data in Marino et al. (2002b).

The data set by Marino et al. (2002b) is the most homogeneous one of all those reported here. We have fitted the relevant data, finding the relation

$$p = 1.2 \times 10^{-3} T_6^{5.2} \quad (3)$$

shown as a dashed line in all the graphs in Figure 6 (T_6 is the temperature in units of 10^6 K); more precisely, the power index found from the fitting is 5.2 ± 0.3 . It is quite interesting that all the stars, the solar corona during the cycle, and the various coronal structures follow this law, which shows a rather steep

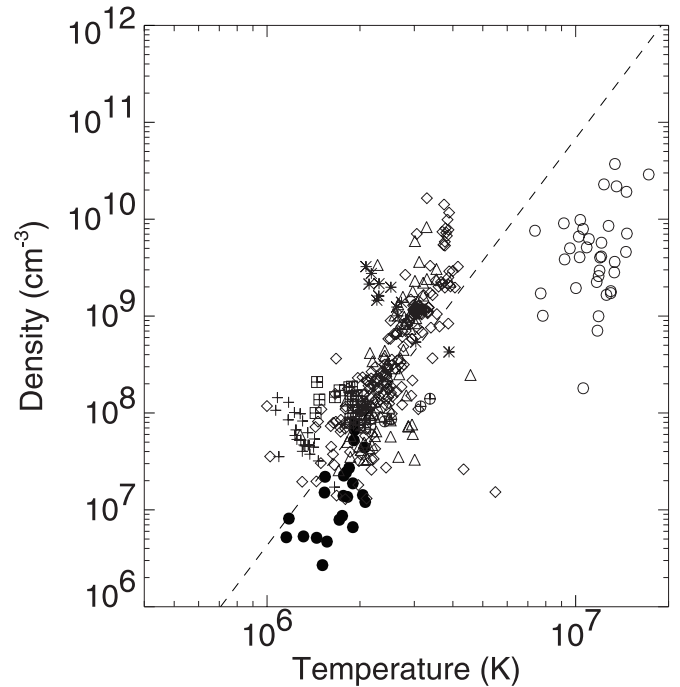


FIG. 7.—Density-temperature diagram of the stellar and the solar data presented in Fig. 6. The dashed line is the $n = 4.3 \times 10^6 T_6^{4.2}$ power law derived from the $p \propto T^{5.2}$ power law and from the ideal gas law for the plasma. Symbols are the same as in Fig. 6.

dependence of the confined plasma pressure on the plasma temperature, probably governed by the heating mechanism(s) due to the magnetic field dissipation. Flares appear to depart, to some extent, from such a law; more specifically, there appears to be a flattening of the pressure-temperature relation with slightly lower pressure than that predicted by the above scaling law.

The diagonal strip covered by the solar corona at various phases and by solar coronal structures is a coarse but firm relation between average pressure and temperature of the loops at different evolutionary stages of the solar structures they form, from emergence to decay. There is a strikingly analogous relation for stellar coronae at different activity levels.

Steady loop models cannot be applied to the rise phase of flares. However, they can be applied, with caveats, to flares during the slow evolution of the decay phase. Because of this, the pressure values corresponding to solar flares are less precise than all the others and have to be taken with care. Indeed, the large spread of solar flare related points suggests the limits of using RTV78 scaling laws on flares.

We also note that the pressure values of the solar structures appear slightly lower than the values predicted according to equation (3); we should note, however, that the surface considered in the *Yohkoh* SXT image is invariably not uniformly filled with loops. Therefore, the local X-ray flux (and the average pressure) is higher than what we measure, even for the solar structures. Determining in detail the area really filled with loops from each *Yohkoh* SXT image is a formidable task. We note in passing that this choice simply skips on the problem of the surface filling factor by coronal structures, probably present also below the angular resolution (see, however, the Appendix).

An equivalent, albeit slightly different, form of the same relation is shown in Figure 7 where we show the average density versus temperature, derived with the ideal gas law for a

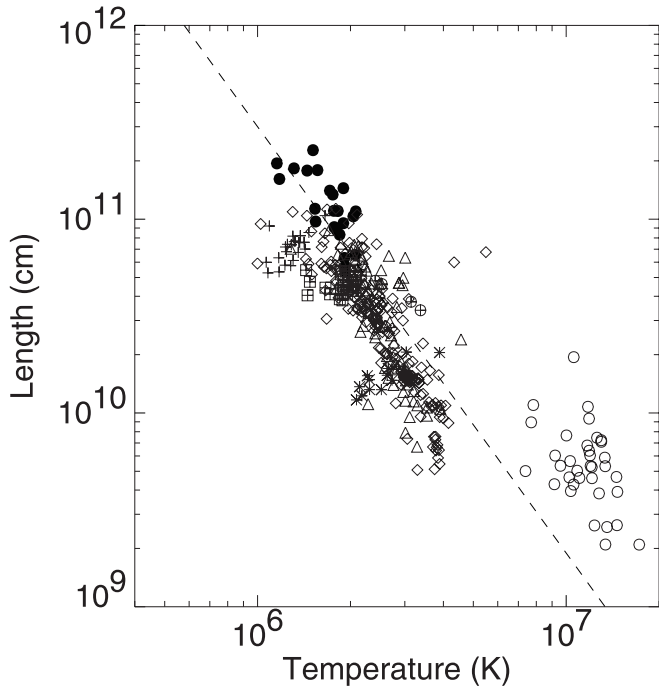


FIG. 8.—Characteristic structure length vs. plasma temperature for the data in Figs. 6 and 7, derived with the RTV78 scaling laws. The dashed line marks the $L = 3.0 \times 10^{11} T_6^{-2.2}$ power law. Symbols are the same as in previous figures.

fully ionized hydrogen plasma $p = 2nk_B T$, where n is the hydrogen number density and k_B is the Boltzmann constant. In this figure we have put together all the solar and the stellar data; obviously, we find

$$n = 4.3 \times 10^6 T_6^{4.2}. \quad (4)$$

Using the RTV78 scaling law 2 and substituting the p - T relation found above, it is straightforward to translate these graphs and laws into the analogous ones relating the characteristic structure length (L) versus temperature (T). Figure 8 shows a graph for the same data as above; the L - T scaling is

$$L = 3.0 \times 10^{11} T_6^{-2.2}. \quad (5)$$

Analogously, substituting equations (3) and (5) into the scaling law (1) we obtain the relation

$$E_H = 1.1 \times 10^{-8} T_6^{7.9} \quad (6)$$

shown as a dashed line in Figure 9, which also shows the same solar and stellar data in a E_H versus T graph.

Flares appear to depart from all the above scaling laws and, in particular, to yield a lower volumetric heating than predicted by the above scaling law, as an implication of the departure from the pressure-temperature scaling law. This may just be an implication of the nonstationarity of the relevant X-ray emitting plasma. However, since many such data are related to the decay phase, i.e., when the loops are in quasi-steady conditions and RTV78 scaling laws should be applicable, we should leave open the possibility that there is indeed a difference in the dissipation mechanisms involved in coronal steady loops and flares.

Since dissipation mechanisms tend to connect volumetric heating with the characteristic size, we are motivated to derive

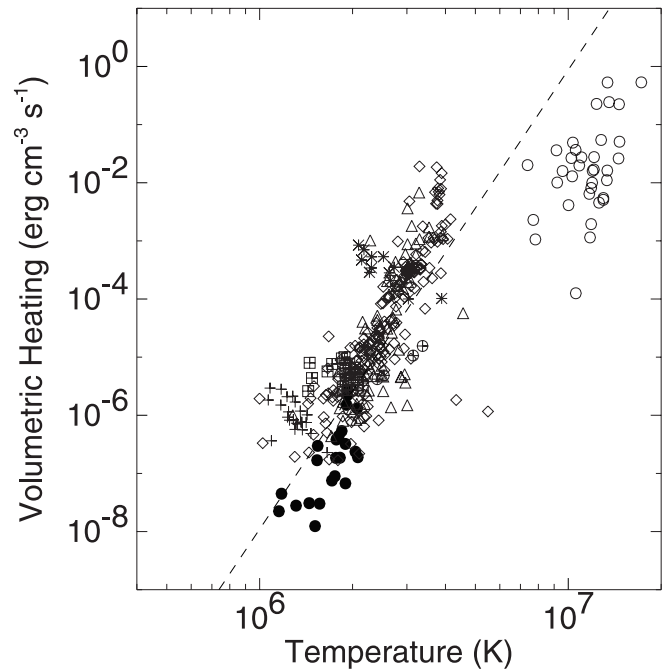


FIG. 9.—Average volumetric heating (E_H) vs. temperature for the data in Figs. 6 and 7 derived with the RTV78 scaling laws. The dashed line marks the $E_H = 1.1 \times 10^{-8} T_6^{7.9}$ power law. Symbols are the same as in previous figures.

a volumetric-heating versus structure-length law. Combining the above scaling laws we find

$$E_H = 1.7 \times 10^{33} L^{-3.6}, \quad (7)$$

also probably dictated by the dispersal and dissipation mechanisms of the magnetic field.

None of the above derivations take into account the fraction of the stellar surface covered by the X-ray emitting region, i.e., the surface filling factor, for clarity's sake. The Appendix contains the generalization of the derivation, considering the surface filling factor.

4. DISCUSSION

4.1. Stellar Coronae Versus the Solar Corona and Its Building Blocks

We have described the coronae of late-type stars of different activity levels as covered by correspondingly different fractions of structures similar to those present in the solar corona. We have classified and grouped these structures as background coronae, ARs, AR cores, and flares, in order of increasing surface X-ray flux and hardness ratio. Indeed, we find the same correlation of F_X versus HR for coronae of late-type stars and for coronal structures present on the Sun. The solar coronal structures, from background corona to large flares, fall in the same region of the F_X and HR diagram where the coronae of late-type stars, from very inactive to extremely active, are located.

The occurrence of a large flare on a star of medium or low activity level should make the star's position in this diagram move toward the right (i.e., with a significant increase of HR) with relatively moderate increase of F_X (Paper II; Orlando et al. 2002). Thus, significant flares in these stars should be very prominent for their variability and because they should make the star move outside the strip covered by coronae.

The most active late-type stars appear to have both F_X and HR significantly higher than even the AR cores, but one can still explain them assuming a significant presence, at any time, of flares or of flarelike structures. Although one cannot exclude the possibility that even moderately active stars may have a contribution due to flares, most of their behavior can be easily explained with ARs. Analogous to the solar case, flares should lead to relatively fast evolution along more horizontal paths slightly departing from the main region of active stars. Many flares may go undetected for a variety of reasons, most likely for the very moderate increase of stellar flux or for the low signal-to-noise ratio of the observation; undetected small flares may, however, lead to a spread along the HR direction of the locus of the stars in the F_X -HR diagram. The diagram in Marino et al. (2002b) containing M stars indeed shows that the M stars are more spread along the HR direction than the G stars; it is quite fitting that M stars are more variable than G stars on short timescales (Marino et al. 2002a).

Only the very late evolutionary phases of AR cores, going toward rather low HR but high surface flux, appear to deviate a little from this scenario. However, the fraction of the surface covered by these very old cores appear to be rather small, and so their emission may be irrelevant with respect to that of the whole stellar corona, as it happens in the solar corona.

4.2. *The Power Laws and a Unified View of the Corona*

The X-ray observations made from *Skylab*, thanks to its several months of coverage, allowed observers for the first time to study the long-term evolution of the X-ray corona (for a review, see Vaiana & Rosner 1978). It became clear that the magnetically confined coronal plasma evolves from the compact, hot, bright, and high-pressure loops of emerging ARs to progressively longer, cooler, dimmer, and relatively low pressure loops, first of ARs and then of the background corona. In this context, therefore, one can also consider the F_X versus HR diagram for solar coronal structures as an evolutionary path. The structures move along the region covered by the various structures, starting with very high F_X , pressure, and temperature and small L , and as they evolve, they get longer and move toward the region with progressively lower F_X , pressure, and temperature.

The various structures of confined plasma, when reported in the pressure-temperature diagram of Figure 6 or, equivalently, in Figures 7, 8, and 9, are all located along a particular track, probably resulting from the physical effects governing the dispersion and dissipation of the magnetic field as it evolves from emergence to total dispersion into background corona. Interestingly enough, this track characterizes both individual structures in the solar corona and the solar corona as a whole at different phases of the solar cycle. The global characteristics result from a sort of averaging of the features of all the structures present in the corona, with a weight due to the surface coverage and to the relative brightness. As a consequence, the average conditions of the solar corona at the minimum of the solar cycle are closer to those of the background corona, even if some ARs may be present, and those of the corona at maximum are closer to AR conditions.

The track also describes the global features of the coronae of solar-type stars. While in the solar case we are able to resolve the entire set of structures at the various evolutionary stages, a star instead just yields one data point in such a diagram, which is an average over all the structures present in its corona. The coronal configuration of the solar-type stars, including the Sun, results from the competing effects of emergence of magnetic

field (generated by the dynamo mechanisms inside the star) and the magnetic field dispersal and dissipation in the outer stellar layers; as a consequence, the average values corresponding to each point in the diagram are determined by these competing physical effects. The higher the emergence rate, the more the point characterizing the stellar corona moves toward the high-pressure-high-temperature part of the graph, as we observe for the Sun (Papers II and IV).

In general, stellar coronae should have a complex coronal composition, according to this scenario, with different fractions of their surface covered with compact, hot, and bright coronal loops and possibly with interactions among magnetic fields of different ARs (Drake et al. 2000). A more active star has a higher number of continuously emerging ARs with very effective magnetic field amplification and dissipation mechanisms. We also claim that each star should have a distribution of structures of confined plasma obeying this sort of universal pressure-temperature relationship with loop plasma pressure higher for higher average loop temperatures.

We note that flares appear to behave differently with regard to the pressure-temperature relation and the related heating-temperature scaling law. As mentioned, this may depend on the nonstationarity of the relevant X-ray emitting structures, but since some of the observations pertain to the decay flares phase when the departure from stationarity is small, we should leave open the possibility that heating mechanisms in flares are indeed different from those of steady structures.

However, if each of the structures evolve similarly and are equivalent to solar structures (as we assume), and if the various coronae are just the sum of the same structures, one should detect all the coronae just as a time average of identical coronal structures, thus all with the same characteristics, independent of the number of structures present. So why should a higher emergence rate lead to higher average surface flux and temperature?

On one hand, a higher emergence rate of magnetic structures brings more ARs, and thus more X-ray emitting regions, to the surface per unit time, leading to higher luminosity and average X-ray flux of the star. As for the temperature and HR, the emission measure of an AR and its core are significantly larger around their emergence (Orlando et al. 2004); also, flares in an AR are more frequent after emergence. The unresolved corona approximates the time average of the structures only if the number of structures of various ages visible at any time is large enough to sample all the evolutionary phases from the AR emergence to the “final decay,” including flares. We doubt that a low-activity star has enough ARs to yield a reasonable “average behavior of structures.” Flares make the “poor sampling” effect even worse.

Typically, a “low-activity” star is caught in a nonflaring phase, and if flares occur, they are easily identified and typically analyzed separately from the rest of the observation. Instead, when we observe a very active star, probably one (or more) of its ARs is in some phase of a flare. Indeed, in order to explain the most active stars we need something brighter and hotter than just ARs, most likely flares, at any time (Drake et al. 2000; Paper III).

Even on the most active stars, however, we may not get a large enough number of ARs to adequately sample the various flare phases, even though we may observe enough ARs to sample (and average) their nonflaring evolution. The stars in the highest part of the F_X -HR diagram appear to vary somehow from one observation to the other (G. Micela 2004, private communication). The locus identifying each

very active star in the diagram may wander around a bit, probably because of flares; the centroid of the stars' loci at any time may yield the average star behavior, and their spread relative to the centroid may yield the stellar variations, apart from experimental uncertainties and stellar peculiarities. The invariable presence of flares probably makes a further significant difference between less active and very active stars.

For completeness we should consider at least two additional effects: (1) a large number of ARs may subtract a substantial amount of surface to the faint, diffuse, structures, so the corona is slightly biased toward higher temperatures and brightness with respect to the average of the structures' evolution that we would see on the Sun; and (2) as mentioned above, if the AR crowding is substantial, ARs may interact, triggering even more flares than expected from just a sum of solar structures.

We have shown that we are able to explain the correlation of F_X versus HR of late-type stars' coronae present in the data of S97 and all the scaling laws we have derived, as due to the plasma structures making up the coronae. Now the focus moves to explaining why X-ray-emitting solar structures follow that very relationship, a task that probably should be accomplished within solar physics and should address the mechanisms governing magnetic field dispersal and dissipation.

We acknowledge useful suggestions by E. Franciosini, A. Maggio, A. Marino, G. Micela, J. Sanz-Forcada, S. Sciortino, B. Steltzer, and an anonymous referee who helped to improve the paper. This work was partially supported by Agenzia Spaziale Italiana and by Ministero della Istruzione, Università e Ricerca.

APPENDIX

GENERALIZATION OF THE GLOBAL SCALING LAWS TO INCLUDE THE FILLING FACTOR

While in the text we have derived the stellar X-ray surface flux by dividing the stellar X-ray luminosity L_X by the stellar surface S_* , a more correct derivation of the X-ray surface flux at the star should consider that only the area A on the star may be covered by coronal structures. Therefore, the whole X-ray luminosity should be $L_X = AE_H L$, and so the surface flux we have derived should include a surface filling factor $F_X = L_X/S_* = AE_H L/S_* = fE_H L$, where f , the surface filling factor, is the fraction of the stellar surface covered with coronal structures.

Therefore, we would obtain $F_X = fpT^{1/2}$, and so would have to relate the fp product with temperature rather than pressure alone. Then equation (3) would become $fp = 1.2 \times 10^{-3} T_6^{5.2}$, and we would obtain $fn \propto T^{4.2}$, $L/f = 3.0 \times 10^{11} T_6^{-2.2}$ instead of equation (5), and $f^2 E_H = 1.1 \times 10^{-8} T_6^{7.9}$ instead of equation (6).

REFERENCES

- Brickhouse, N. S., Dupree, A. K., & Young, P. R. 2001, *ApJ*, 562, 75
- Drake, J. J., Peres, G., Orlando, S., Laming, J. M., & Maggio, M. 2000, *ApJ*, 545, 1074
- Favata, F., Reale, F., Micela, G., Sciortino, S., Maggio, A., & Matsumoto, H. 2000, *A&A*, 353, 987
- Favata, F., & Schmitt, J. H. M. M. 1999, *A&A*, 350, 900
- Franciosini, E., Pallavicini, R., & Tagliaferri, G. 2001, *A&A*, 375, 196
- Guedel, M., Audard, M., Skinner, S. L., & Horvath, M. I. 2002, *ApJ*, 580, 73
- Guedel, M., Guinan, E. F., & Skinner, S. L. 1997, *ApJ*, 483, 947
- Jordan, C., & Montesinos, B. 1991, *MNRAS*, 252, 21P
- Judge, P. G., Solomon, S. C., & Ayres, T. R. 2003, *ApJ*, 593, 534
- Kaastra, J. S. 1992, An X-Ray Spectral Code for Optically Thin Plasmas (Internal SRON-Leiden Rep., updated ver. 2.0)
- Maggio, A., Pallavicini, R., Reale, F., & Tagliaferri, G. 2000, *A&A*, 356, 627
- Marino, A., Micela, G., Peres, G., & Sciortino, S. 2002a, *A&A*, 383, 210
- Marino, A., Peres, G., Micela, G., & Sciortino, S. 2002b, in ASP Conf. Ser. 277, *Stellar Coronae in the Chandra and XMM-Newton Era*, ed. F. Favata & J. J. Drake (San Francisco: ASP), 539
- Mewe, R., Kaastra, J. S., & Liedahl, D. A. 1995, *Legacy*, 6, 16
- Mewe, R., Lemen, J. R., & van den Oord, G. H. J. 1986, *A&AS*, 65, 511
- Micela, G. 2002a, in ASP Conf. Ser. 269, *The Evolving Sun and Its Influence on Planetary Environments*, ed. B. Montesinos, A. Gimenez, & E. F. Guinan (San Francisco: ASP), 107
- . 2002b, in ASP Conf. Ser. 277, *Stellar Coronae in the Chandra and XMM-Newton Era*, ed. F. Favata & J. J. Drake (San Francisco: ASP), 263
- Orlando, S., Peres, G., & Reale, F. 2000, *ApJ*, 528, 524 (Paper I)
- . 2001, *ApJ*, 560, 499 (Paper IV)
- . 2002, in ASP Conf. Ser. 277, *Stellar Coronae in the Chandra and XMM-Newton Era*, ed. F. Favata & J. J. Drake (San Francisco: ASP), 341
- . 2004, *A&A*, in press
- Pallavicini, R., Golub, L., Rosner, R., Vaiana, G. S., Ayres, T., & Linsky, J. L. 1981, *ApJ*, 247, 692
- Peres, G., Orlando, S., Reale, F., Rosner, R., & Hudson, H. 2000, *ApJ*, 528, 537 (Paper II)
- Preibisch, T. 1997, *A&A*, 20, 525
- Reale, F., Peres, G., & Orlando, S. 2001, *ApJ*, 557, 906 (Paper III)
- Rosner, R., Tucker, W. H., & Vaiana, G. S. 1978, *ApJ*, 220, 643 (RTV78)
- Schmitt, J. H. M. M. 1997, *A&A*, 318, 215 (S97)
- Schmitt, J. H. M. M., Collura, A., Sciortino, S., Vaiana, G. S., Harnden, F. R., Jr., & Rosner, R. 1990, *ApJ*, 365, 704
- Schmitt, J. H. M. M., & Favata, F. 1999, *Nature*, 401, 44
- Schrijver, C. J., Mewe, R., & Walter, F. M. 1984, *A&A*, 138, 258
- Schrijver, C. J., & Title, A. M. 2001, *ApJ*, 551, 1099
- Steltzer, B., 2001, Poster presented at Joint European and National Astronomical Meeting
- Vaiana, G. S., & Rosner, R. 1978, *ARA&A*, 16, 393
- Vaiana, G. S., et al. 1981, *ApJ*, 245, 163
- Vesecky, J. F., Antiochos, S. K., & Underwood, J. H. 1979, *ApJ*, 233, 987
- Wood, B. E., Linsky, J. L., & Ayres, T. R. 1997, *ApJ*, 478, 745